

Ni₂₁Cr₁₁Al_{2.5}Y₁Co COMPOSITE COATED CARBON STEEL TESTED IN GEOTHERMAL CONDITIONS

Aurelian BUZAIANU^{1*}, Sigrun KARLSDOTTIR², Kolbrun RAGNARSDOTTIR³, Helen HARALDSDOTTIR³, Saemundur GUDLAUGSSON⁴, Petra MOTOIU⁵, Ioana CSAKI⁶

¹ Metav- R&D, Bucharest, 31 C.A.Rosetti St., 020011, Romania.

² Mechanical Engineering at the University of Iceland.

³ Innovation Center Iceland-ICI, Arleyinir 2-8 Reykjavik, Iceland.

⁴ Orka Náttúrunnar; 110 Baejarhals, Iceland.

⁵ Tehnoid Com Ltd., 48 Baritiu St, 011295, Romania.

⁶ "Politehnica" University Bucharest, 313, Splaiul Independentei; 60042, Romania.

Abstract

This study aims to review in situ corrosion tests and evaluated some characteristics of complex composite layers based on powders Ni₂₁Cr₁₁Al_{2.5}Y₁Co with 3%WC. These powders presenting agglomerate WC nan-sized cluster particles and are used as an option for coating geothermal carbon steel components to prevent extensive erosion-corrosion phenomenon. The powders are used to protect steel components by multilayer thermal spraying HVOF deposition. The experimental procedure involved obtaining X-ray diffraction patterns of the specimens, profilometry images of erosion-corrosion tests and SEM investigation to provide detailed information about adhesion of protective layers and morphological modifications.

Keywords: multi-layer composite, powder plasma deposition, geothermal power plants.

Introduction

In the geothermal power plant, the corrosion and erosion process take place continuum and the phenomena it depends on the geothermal steam enthalpy, pressure, chemical composition of the impurities carried by the geothermal water vapor and their steam treatment. The damage due to the erosion-corrosion has long been recognized as a major cause of reducing the functionality of geothermal power plants [1]. In order to increase the reliability of geothermal power plant, it is important to evaluate and extend the life of the materials that operate in the geothermal environmental conditions [2, 3]. The most common corrosion problems occur due to high content of non-condensable gases from geothermal steam where we find:

- a high content of H₂S that generates metallurgical problems such as corrosion, fatigue and tendency toward friability of steel, which leads to failure of the turbine components;
- a high CO₂ content in the geothermal liquid which at about 200°C accelerates the formation of calcite, resulting in a strong corrosion of the turbine components;
- sulfur deposition due to the high content of gases that are found in the base composition of geothermal steam;
- corrosion due to low pH and variable oxygen content in the components that are circulating with the geothermal steam.

* Corresponding author: buzaianu@metav-cd.ro

The content and composition of the solid component varies; normally can be found chloride and various different types of elements, as for example the geothermal fluid with fluorine or boron. Values that tent to 130g/kg appear, the largest item being the content of sodium chloride. For example, in Iceland, the total dissolved solid content is approximately 30g/kg respectively and can be found in

Svartsengi area [4], and the gas content of the geothermal steam reservoirs is substantial as shown in Table no.1.

Table.1. Examples of chemical composition of non-condensable gases of the current reservoirs systems of medium and high enthalpy used in geothermal power plants (Iceland).

Geothermal reservoir (depending on extraction areas)	Pressure [atm]	H2O [%]	CO2 [%]	H2S [%]
Reykjanes	10, 0	99, 30	0, 672	0, 019
Svartsengi	5, 5	99, 80	0, 196	0, 003
Hveragerdi	5, .5	99, 84	0, 138	0, 006
Bjarnarflag	11, 0	99, 70	0, 060	0, 060
Krafla	8	98, 70	1, 140	0, 070

As a result of the matters presented, the most serious problems occurring in geothermal power plants are due to accentuated carbon steel corrosion as a result of the content of existing corrosive agents in the geothermal steam used [5] These contamination components of the steam induce in the steels components: erosion and corrosion, fatigue corrosion under tension, as well as micro cracks and fracture, due to the embitterment of the steel caused by presence of hydrogen [6] At the same time there are taking place other effects that occur on a microscopic scaled which due to their accumulation emphasizes the degradation and deterioration of materials as a result of the direct action of chemical agents mentioned [7, 8]. In addition it appears extend area corrosion, which in geothermal steam conditions can be defined as a accelerated corrosion, occurring as a result of the presence of contaminants as salts [9] Especially hot corrosion occurs when metals are heated in the temperature range of 220-350°C, in the presence of sulfate deposits formed as a result of the reaction between sodium chloride and sulfuric compounds of the metallic turbine structure components. At high temperatures, the deposits of Na₂SO₄ and NaCl in solutions, causes accelerated attacks in steels. This type of attack represents an accelerated corrosion that may be caused also by the existence of other combined salts or sulfurs in the solid solutions or liquids associated with the no condensable gases explained in Table no.2.

Table.2. Examples of chemical compositions for geothermal no condensable gases from a geothermal power plant - Hellisheiði Iceland (Geothermal steam enthalpy is 170 °C at 6.7 bar).

Noncondensable Gas	H ₂ (mg/kg)	N ₂ (mg/kg)	CH ₄ (mg/kg)	H ₂ S (mg/kg)	CO ₂ (mg/kg)
Turbine 1	31.14	28.85	4.43	804.3	1864.6
Turbine 2	23.78	32.45	6.17	741.9	3087.2
Turbine 3	29.35	22.71	5.05	929.0	2261.8

Experimentally it has been found that the erosion-corrosion process can be slowed by using new materials, who have a good chemical control of the destructive action of geothermal steam, just by creating new types of surfaces and redesigned carbon steel materials for: condensers, pumps, gas extraction pipe system and turbine diafragms. Due to their specific physic-mechanical and chemical properties of nanosized WC powders components, have become one of the key solution of layers composite components to protect steel geothermal components. The in situ studied of composite layers protection, are the good option for improvement the erosion of steel and for corrective test action to prevent corrosion and will enable to reduce the consumption of corrosion resistant alloys.

Materials and Methods

These protection surfaces can be achieved by using multicomposite type materials which can be ceramic or metal-ceramic powders [10, 11]. To find the optimal coating, it is necessary to have a good understanding of the operating conditions. Thermal spraying High Velocity Oxidation Fuel Deposition (HVOF) has emerged as a suitable technique [12, 13] and is widely used to apply wear, abradable and corrosion protective composites coatings for metallic components and application in geothermal conditions. The plasma coatings, are relatively heterogeneous, no isotropic, micro porous and contain micro cracks[14]. The literature is mentioning that adherence of the sprayed particles occurs, in generally by a mechanical adherence, simultaneously with the attachment of particles during their cooling and contracting, as well as other physical adhesion processes [15]. Thermal plasma HVOF deposition coatings form the stable oxides with low diffusion coefficients for oxygen. Thermal spraying was undertaken using a metalization HVOF jet, using propane and oxygen gases under variable pressures. After combustion the gases flow a high speed through a nozzle beyond where the powder is injected by a carrier gas through the samples. In this context pre-alloyed metallic compounds with controlled particle morphology can be useful in assisting composite homogenization and densification. Commercial metal powders were purchased from Sulzer Metco (Table no.3) including Cr (7-12µm-99.5% pure); Ni (4-8µm-99.5% pure); Al (4.5µm-97.5% pure). The powder components were weighted according to the designed composition, and initially are mechanically blended. Chemical composition of the hard particles is 99.9% W pure, apparent density is 18.5g/cm³ and particle size diameters are maximum 800nm. The tungsten particle size affected the morphology and mixing homogeneity of complex composites. The presence (Table no.4) of nanoscale WC grain size (500-800 nm) can be beneficial an increase of abrasive and sliding wear resistance of complex protective composites coatings.

Table 3. Chemical composition of the base complex powders.

Elements	Ni	Cr	Al	WC	Y	Co
Composition (wt %)	base	21	11	3	2.5	1

Table 4. Feature of the characteristics of complex powders.

Characteristics of powder	Apparent density	Flow rate	Granulometry
Ni21Cr11Al2.5Y1Co with 3%WC	4.5g/cm ³	3.4s/50g	-43/+20µm (mesh -330/+20µm) 500-800nm

Complex matrix of Ni-Cr-Al-Y-Co powders and 3%WC hard particles have been used as alternative composite coatings. In the presence of Al, NiAl compounds appear and coatings exhibit system performance and excellent carburization resistance at high temperature. The presence of carbon in the complex powder produces hard carbides, with increased hardness resulting in high wear resistance of the coatings. Atomizing process is rounded to spherical in shape with relative smooth surfaces and the apparent density of the matrix is 4.5 g/cm^3 . Chemical composition of the hard particles is 99.9% W pure and 500-800 nm particle size diameters.

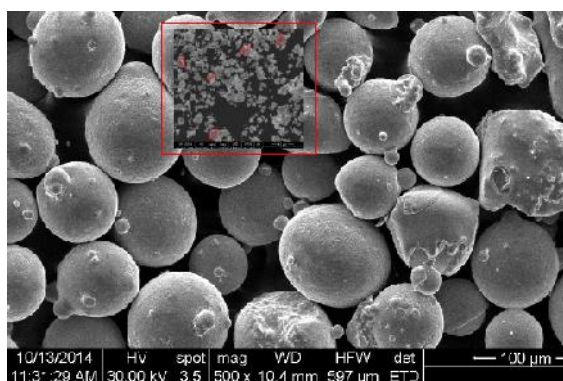


Fig.1. SEM micrography of the complex Ni-Cr-Al-Y-Co powders.

In SEM image the particle shape and surface topography can be observed. Gas-atomized are rounded to spherical in shape (Figure 1) with relative smooth surfaces and medium particles size are $65 \mu\text{m}$. The spheroidization is detected and we can see a significant increase of equivalent diameter (Table 4). The relative occurrence of the dimensions has been found to depend of the distributed of elemental powder on the particle surfaces). The effect of decreased particle size on density is particularly significant (apparent density 4.5 g/cm^3) for particle sizes of then $20 \mu\text{m}$ (Table 4). Presence of WC depresses the melting temperature and contributes to the formation of hard phases.

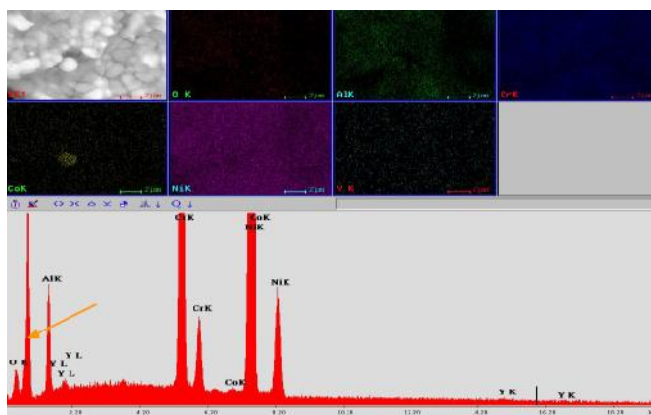


Fig.2. EDX mapping micrography of the complex Ni-Cr-Al-Y-Co matrix powders.

In the EDX spectrum (Figure 2) was observed with low intensity and broadened width, indicating that Y₂O₃ particles into the complex-powders samples. In this powders case, the RDX analysis (Figure 3) is a technique for the rapid determination for samples homogeneity degree. This analyze displays the spectrum of composition existing in a given inhomogeneous phases from the shape of diffraction peak broadened by a range of lattice phase parameters.

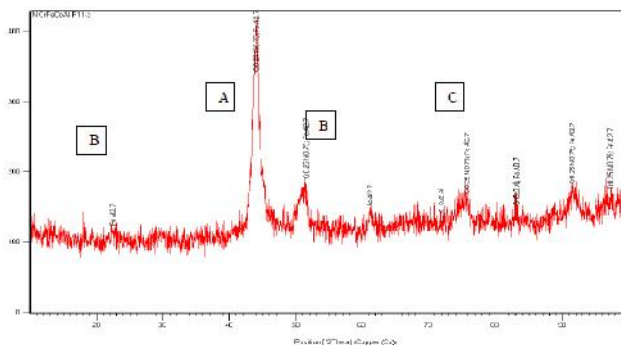


Fig.3. Indexing of the X-ray diffraction pattern of textured matrix sample Ni₂₁Cr₁₁Al_{2.5}Y₂O₃1Co after milling and mechanical homogenization (2-Theta, deg).

The major cubic Cr_{0.25}Ni_{0.75} phases (Fig.3-A) and orthorhombic FeAl_{2.7} phases (Fig.3-B) and the minor cubic phase Cr_{0.25}Co₂Al (Fig.3-C) were observed in the samples. The XRD pattern showed the broadened multiple diffraction peaks with low intensity, confirming the crystalline and fine size of the NiAl and the presence of Y₂O₃ components in the composites. The Y₂O₃ improves adherence and appalling resistance of oxide layer, and hence improves oxidation, sulfidation and carburization resistance of surfaces composites. In different manufacturing processes the powder result in different morphology, density, initial phases, particle size distribution and carbide grain size within the powders. Li et al [16] stated that the degree of decarburization during HVOF spraying mainly depends on the type of powder, in particular, the presence of complex carbides (such as W₂C and Co₃W₃C) in the powder. De Villiers Lovelock et al. [17] also reported that a high amount of W₂C in the starting powder generates a larger amount of complex carbide phases in the thermally sprayed coating leading the lower wear resistant coatings. The particle surface to volume ratio also affects the degree of decomposition, with porous particles being prone to overheating. Finer carbide sizes in these powders result in lower surface roughness of the coating Jorosinski et al., [18]. Powder with a spherical morphology has excellent flow ability and feed ability through the system. B. Wang et al [19] stated that the fused and crushed WC-Co powder, which has an angular shape, did not flow continuously when sprayed with HVOF (JP-5000). The shape of powder affects the flow rate; as a result, very low deposition rates for angular powders are commonly observed. The parameter of process deposition and general condition regarding gas and flows pressures are thus suggested in the Table 3.

Table 3. Feature of the characteristics of experimental HVOF samples deposition.

Gas	Volume flow [SLPM]*	Operating pressure [MPa]
Oxygen	250-350	1.0
Propane	40-80	0.05
Air	450-600	0.07

* *SLPM* = Standard Liters per Minute Gas consumption.

Results and Discussion

HVOF system, which can provide high-velocity gas jet with significantly lower heat flux, is an alternative to plasma technologies. High power of the gas jet has a dominating kinetic component. Powder in these jets acquire high kinetic energy without powder. This can form a lamella coating structure on a hard substrate. In the Figure no.4 is presented the HVOF gas supersonic jet and the formation phenomena of stationary shock waves in plasma process deposition of layers on the disc specimens used for the In-situ tests corrosion in geothermal steam.

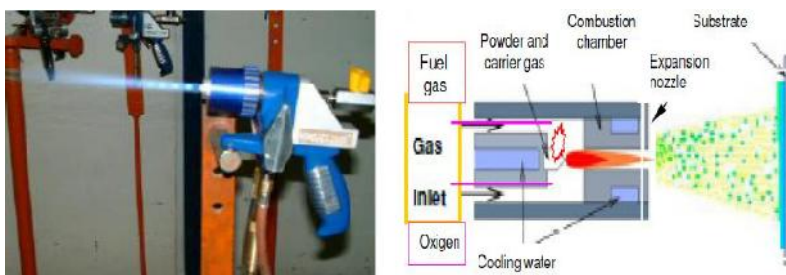


Fig.4. Plasma HVOF process and schematic representation of the components of plasma jet metalizing device deposition system.

To obtain continuum metallic layers on the surface of the disks steel samples specimens (Figure no.5a), they were mounted on a specially constructed device, because they can move in a continuous motion rotary head toward the gun process deposition. The device built allows a uniform movement through a constant rotation of specimens. Movement is done with a rotating head grip that allows a controlled deposition of material layer by layer over the entire surface and exposed them for the entire operation period of discs samples depositions ((Figure no.5b).

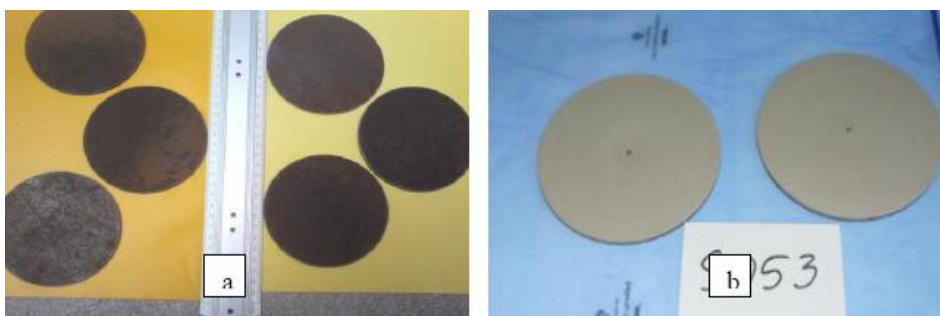


Fig.5. Shows the steel disks surface preparatory (a) and after to plasma HVOF experiment process (b). Diameter of disks 106mm.

The control of porosity is critical (Figure no.6) to obtain the performance of any erosion-corrosion control and the spray distance is an important parameter to be considered for tuning the processing conditions and thus to maintain or even improve [20] the adhesion of the coatings. To increase the adherence between the layers, a NiCr 80/20 primary layer seems better to use.

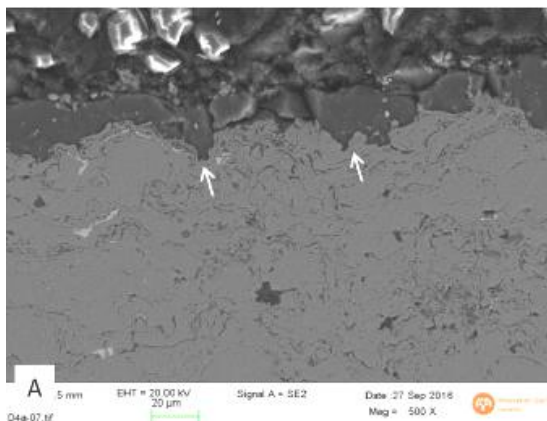


Fig.6. Cross-sectional view using SEM. Figure shows were V-shaped holes are forming indicated by white arrows.

Any defects that allow ingress of aggressive species will accelerate the coating-degradation process. Much attention has been paid to the control and modification of porosity. In this study, the porosity of HVOF spray was classified according to the potential mechanism of formation of diverse type of porosity. The test setup is attached to a geothermal wellhead and furthermore simulates the environment in component turbines, where high-velocity collisions with hard particles and water droplets erode steel surfaces of the turbine parts. The setup (Figure no.8 and 9) is connected to the well HE-29 of the Hellisheidi–Iceland geothermal power plant, which was considered suitable for simulation of the steam environment in a steam geothermal turbine. Well HE-29 has wellhead temperature around 220°C and wellhead pressure around 18 bars and the steam velocity around 31m/s. Erodent impact angle of steam components is 90° on the steel plate sample.

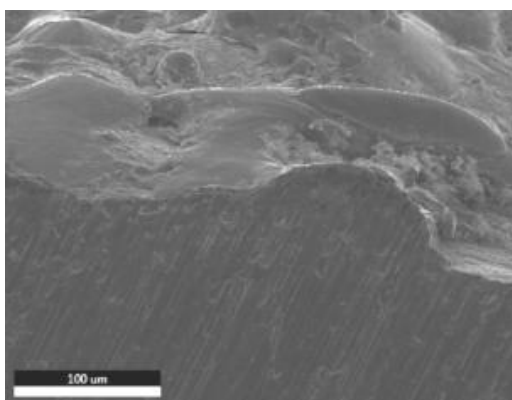


Fig.7. SEM image of the final surface. The final surface shows: no porosity and cleavage direction and no intergranular composite micro-crakes.

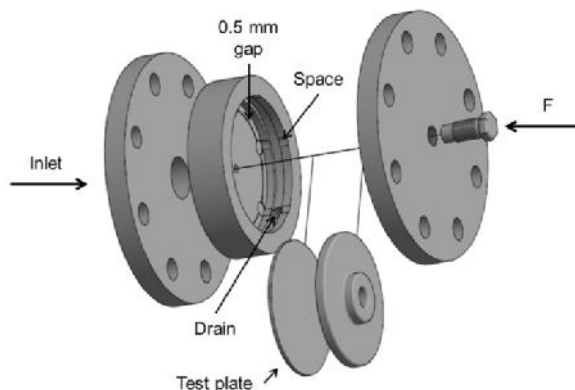


Fig.8. A scheme of setup test unit holder s of steel carbon plate with protective layers.



Fig.9. Detail of the mechanical components of the experimental equipment system (test unit holder).

The setup was designed so that steam flows directly from the wellhead into the In-situ test unit, through a nozzle where the steam is flashed on the target area, simulating the effect of erosion and erosion-corrosion in geothermal power plant. To tests the chosen distance between the nozzle opening and the sample plate was 0.5 mm, which gave erosion of 350-400 μm of low-carbon sample steel after 30 days exposure to steam. The Figure no.10 is a view of test In-situ equipment connected to the well HE-29 of the Hellisheiði geothermal power plant.

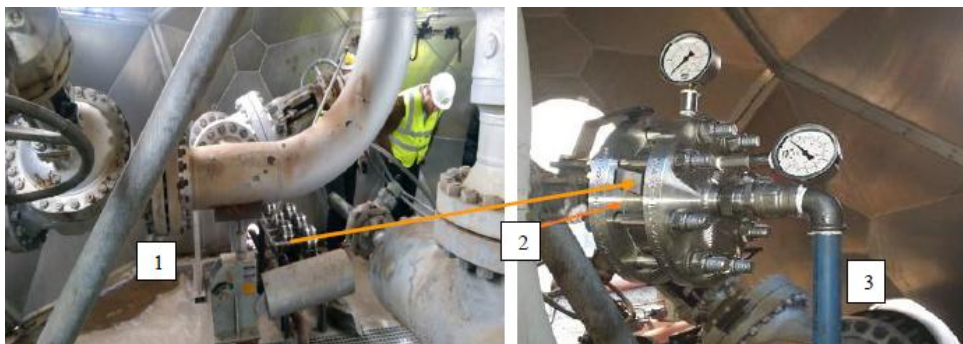


Fig. 10. Test setup connected to the well HE-29 head (1) Hellisheiði -Iceland indicating the positions of samples (2) and steam control and evacuation (3).

At the visual inspection of the discs, the droplets erode composite steel surfaces of the samples and the eroded area is positioned from the central point of the plate. Some degree of erosion is directly visible on most samples. In many cases the eroded area is also covered by scaling from the geothermal steam.



Fig.11. The coated test plates after two months of exposure to geothermal steam. Central the eroded area (a) and scaling deposition from the geothermal steam (b).

The un-coated disc samples were analyzed after 30 days exposure to steam to compare the different test runs and to analyzed and observe the general performance of coated and un-coated samples in this environment. For the un-coated carbon steel samples, visual inspection of this disc showed that the scaling was not as evident as for the other samples and erosion appeared to affect a larger area on this sample (Figure no.12). The SEM analysis showed the presence of a uniform corrosion layer covering the top part of the material. This layer was mainly present in the areas which also contained silica scaling. Other forms of corrosion were also present such as pits but they were generally comprised mainly of oxygen and iron.



Fig.12. The un-coated test plates after 30 days of exposure to geothermal steam. Central area is much eroded minor scaling deposition from the geothermal steam.

Figure no.12 shows the un-coated test plates after one month of exposure to geothermal steam. The eroded area is positioned from the central point of the plate. Some degree of erosion is directly visible on most samples, but in many cases the eroded area is also covered by scaling from the geothermal steam. As noted the scaling was brittle and in some areas easily removed.

The erosion effect on the samples was measured through the decrease of the material both with an optical profiler (Figure no.13-Solaris SD-V100 optical 2D scan profiler) and through measurements in the SEM analysis.



Fig.13. Solaris surface profilometer to capture erosion/corrosion image of the samples.

Visual inspection of the samples showed that there was a significant amount of silica scaling on the samples and inspection of the surface in the SEM showed that there was a silica layer covering the whole sample. Silica deposits can be transparent which allow for the optical profiler to reach the surface of the samples through the silica layer in some cases. The results from the optical profiler were therefore used as rough initial estimates of the reduction in thickness. For the un-coated samples the most significantly eroded area is generally around 6-8mm in diameter therefore a 30x30mm area around that area was analyzed (Figure no.14). The reason such a large area was analyzed was to get a better estimate of the reduction in the original thickness. The following image shows an example of the surface depth around the eroded area measured with the optical profiler. The depth of the eroded area can be viewed more quantitatively by observing a cross sectional surface profile through the eroded area. The following images show this profile for discs.

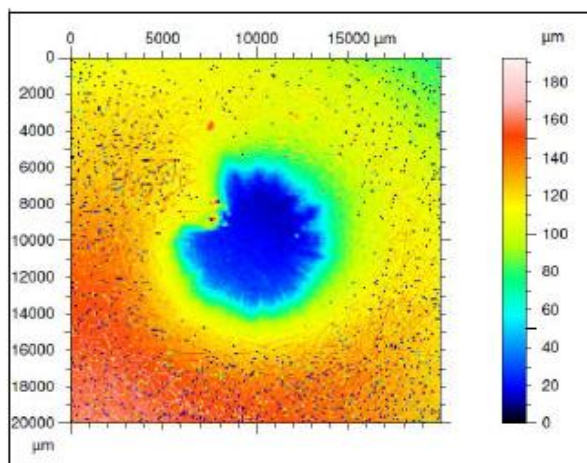


Fig. 14. The surface of sample un-coated disc measured with the optical profiler.

For the coated disc, the cross-sectional profiles show as in Figure no.15. The profiler's view of the coating surface is obstructed by deposits. This was most pronounced in the central area, where no one reliable measurement of the erosion depth could be obtained.

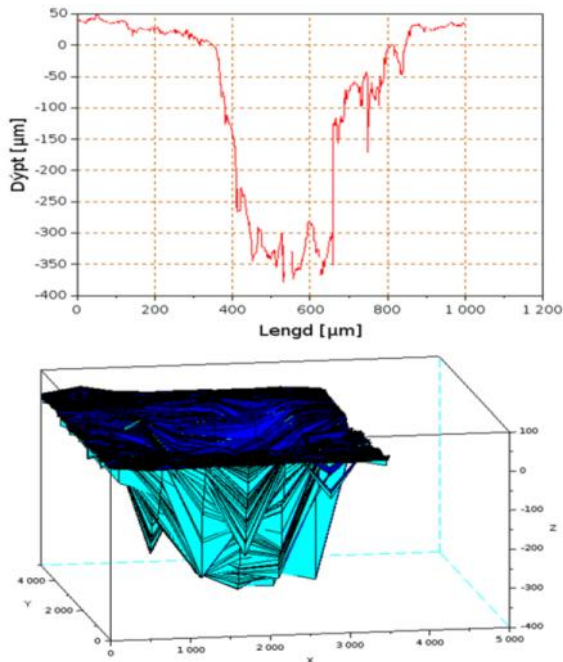


Fig. 15. The central area profiler surface of sample coated disc measured with the optical profilometer.

The SEM analysis and Figure no.16 shows where the chemical compositions shown in Table 6 were measured, indicated by white boxes.

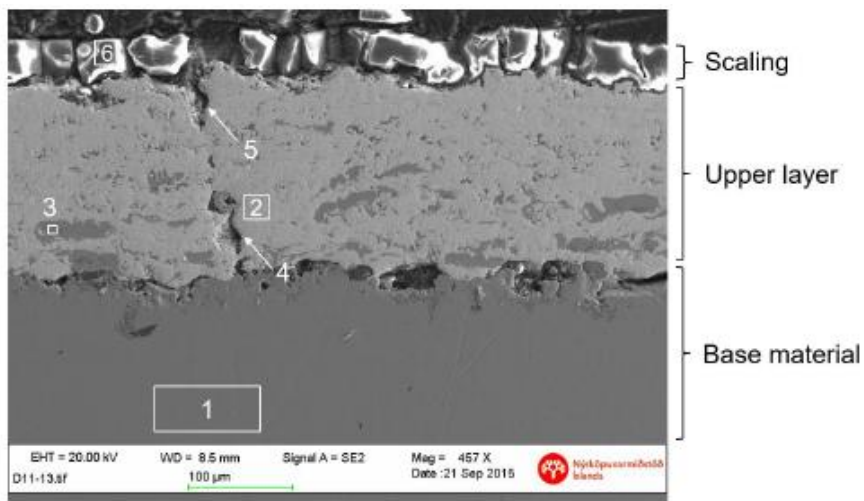


Fig.16. Cross-sectional view of the of sample coated disc using SEM. The figure shows uniform corrosion.

Table 6. Chemical composition of the corresponding areas on disc. All of the results are given in Wt%. The scaling surfaces of the disk consisting of silica with small amounts of Al and Na, Ca, K corrosion steam components.

Location	C	O	Fe	Al	Si	Cr	Co	Ni	W	Mn	K	Ca	Na	Br
1: base			98.2							0.58				
2: coating/bulk	0.79	1.38	0.51			3.36	8.56		81.53					
3: coating/inclus'n		1.44	2.73		3.82	9.75		82.3		0.92				
4: crack-bottom	2.61	16.37			1.26	3.70	26.28	4.02	31.34					
5: crack-top	9.99	20.21			1.37	2.46	6.35		46.22			0.77	0.34	1.99
6: scaling		53.25	0.58	5.13	34.79				1.31	0.30	1.62	1.88	1.68	

Analysis of the interface region between the bond coating and the base material reveals the existence of Fe and O, which could indicate the presence of corrosion products due to corrosion occurring between the coating the base material. There is visible discontinuity in the area 4-5 that could allow access of steam to that location; it is possible that it is a contamination from the production of the coating. Certainly important microstructure layers deposition of multilayer composite, especially for corrosion-control applications, require a continuum barrier to stop of conducting corrosive liquids, that no include porosity and micro cracks.

Conclusion

From the present study we can draw the following conclusions:

- HVOF is a suitable technique for applying coating layers with wear and corrosion resistance. The HVOF makes it possible to produce Ni₂₁Cr₁₁Al_{2.5}Y₁Co thermal coating deposition layers with 3%WC hard particles that create phases with complex chemical composition.

- Typically we need to add Cr, which forms the Cr₂O₃ layer. The Fe oxides are a good oxygen conductor, which diffuse through the top coat and assist in the formation of the Cr₂O₃ coat. The major cubic Cr_{0.25}Ni_{0.75} and orthorhombic FeAl 2.7 phases and Cr_{0.25}Co₂Al were observed in the multilayer samples.

- The XRD spectrum confirms the crystalline and fine size of NiAl and Y₂O₃ components in the composites. These components improve adherence and resistance of oxide layers and hence improve oxidation, sulphidation and carburization resistance of surface layers.

- Finer carbide sizes in these powders result in good abrasive wear and lower surface roughness of the coating. The presence of WC in the starting powder generates a larger amount of complex fine carbide phases in the HVOF coating leading to the lower resistant corrosion coatings.

- In-situ tests, the erosion & corrosion resistance of the tested coated sample discs by HVOF spraying is about 70% higher than that of the uncoated carbon steel sample.

Acknowledgements

This work is supported by the Grant Romanian EEA Financial Mechanism Committee 2009-2014 and Iceland as Donor Stat. Bilateral Agreement Program 2014-2017 Iceland-Romania „Research within priority sectors”. Contract 16 SEE /30.06.2014.

References

- [1] R. Adiprana, E. Yuniarto, G. Salak, *Geothermal Power Plant Experience of Scaling/Deposit: Analysis, Root Cause and Prevention*, **Proceedings World Geothermal Congress, 2010, Bali, Indonesia**.
- [2] S.N. Karlsdóttir, **Comprehensive Renewable Energy**, ElsevierLtd., 2012, pp. 239-257.
- [3] S.Yoshihiro, O.Yoshiki, Hideo Kato, *The Latest Geothermal Steam Turbines*, **Fuji Electric Rev**, 55, 3, 2011, pp. 38.
- [4] E.T. Eliassonm, *Power Generation Nationalfrom High-Enthaply Geothermal Resources. EnergyGHC Bulletin Authority*, **Reykjavik, Iceland.**, June 2011.
- [5] H.A. Alfredsson, E.H. Oelkers, B.S. Haráarson, H. Franzson, E. Gunnlaugsson, S. Gislason, *The geology and water chemistry of the Hellisheidi, SW-Iceland carbon storage site*, **International Journal of Greenhouse Gas Control**, 12, 2013, pp. 399-418.
- [6] M. Stapleton, *Scaling and Corrosion in Geothermal Operation*. **Power Chem Technology**, 1, 2002, pp. 15-18.
- [7] R.Corsi, *Scaling and Corrosion in Geothermal Equipment: problems and preventive measures*, **Geothermics**, 15, 5-6, 1986, pp 839-856.
- [8] A. Stefansson, S. S. Arnórsson, I. Gunnarsson, H. Kaasalainen and E. Gunnlaugsson, *The geochemistry and sequestration of H₂S into the geothermal system at Hellisheidi, Iceland*, **Journal of Volcanology and Geothermal Research**, 202, 3-4, 2011, pp. 179-188.
- [9] R. Adiprana, E. Yuniarto, G. Salak, *Geothermal Power Plant Experience of Scaling/Deposit: Analysis, Root Cause and Prevention*, **Proceedings World Geothermal Congress 2010 Bali, Indonesia**, 25-29 April 2010.
- [10] S. Kamal, R. Jayaganthan, S. Prakash, Evaluation of cyclic hot corrosion behaviour of detonation gun sprayed Cr 3C 2-25%NiCr coatings on nickel- and iron-based superalloys, **Surface & Coatings Technology**, 203, 8, 2009, pp 1004-1013.
- [11] S. Chatha, H. S. Sidhu, B. S. Sidhu, *Characterization and Corrosion-Erosion Behavior of Carbide based Thermal Spray Coatings*, **Journal of Minerals & Materials Characterization & Engineering**, 11, 6, 2012, pp. 569-586.
- [12] J. A. Cabral-Miramontes, C. Gaona-Tiburcio, F. Almeraya-Calderón, F. H. Estupiñan-Lopez, G. K. Pedraza-Basulto, 1 and C. A. Poblano-Salas, *Parameter Studies on High-Velocity Oxi-Fuel Spraying of CoNiCrAlY Coatings Used in the Aeronautical Industry*, **International Journal of Corrosion**, 2014, 2014, pp 1-8, Article ID 703806. doi.org/10.1155/2014/703806.
- [13] R.C. Souza, H.J. Voorwald, M. Cioffi, *Fatigue strength of HVOF sprayed Cr3C2-25NiCr and WC-10Ni on AISI 4340 steel*, **Surf. Coat. Technol.**, 203, 2008, pp. 191-198.
- [14] S. Matthews, B. James, M. Hyland - *Erosion of oxide scales formed on Cr3C2-NiCr thermal spray coatings*, **Corrosion Science** 50, 2008, pp 3087-3094.
- [15] Z. H. Masuku, P. A. Olubambi, J. H. Potgieter, B. A. Obadele, *Tribological and Corrosion Behavior of HVOF-Sprayed WC-Co-Based Composite Coatings in Simulated Mine Water Environments*, **Tribology Transactions**, 58, 2, 2015, pp. 337.
- [16] C.J. Li, A. Ohmori, and Y. Harada, *Formation of an Amorphous Phase in Thermally Sprayed WC-Co*, **J. Therm. Spray Technol.**, 1996, 5, pp. 69-73.
- [17] H.L. de Villiers Lovelock, P.W.Richter, J.M.Benson, P.M.Young, *Parameter Study of HP/HVOF Deposited WC-Co Cotings*. **Journal of Thermal Spray Technology**, 7, 1998, pp. 7-107.

- [18] W.J.Jarosinski, M.F.Gruninger and C.H.Londry, *Characterisation of Tungsten Carbide Cobalt Powder and HVOF Coatings*, **Proc. 5th National Thermal Spray Conf., California, 1993**, pp 153-158.
 - [19] B. Wang, A. Verstak, *Elevated temperature erosion of HVOF Cr₃C₂/TiC– NiCrMo cermet coating*, **Wear**, 233-235, 1999, pp. 342–351.
 - [20] G. Bolelli, L. Berger, H. Koivuluoto, *Tribology of HVOF- and HVAF-sprayed WC-10Co4Cr hardmetal coatings: A comparative assessment*, **Surface & Coatings Technology**, **265**, 2015, pp. 125-144.
 - [21] M.Ahmad, M. Casey, N. Sürken, *Experimental assessment of droplet impact erosion resistance of steam turbine blade materials*, **Wear**, **267**, 9-10, 2009, pp.1605-1618.
-

Received: July 6, 2017

Accepted: September 12, 2017